JOURNAL OF BACTERIOLOGY, Nov. 2005, p. 7518–7525 Vol. 187, No. 21
0021-9193/05/$08.00+0 doi:10.1128/JB.187.21.7518–7525.2005
Copyright © 2005, American Society for Microbiology. All Rights Reserved.

Characterization of Bacterial Drug Antiporters Homologous to Mammalian Neurotransmitter Transporters

Eyal Vardy, Sonia Steiner-Mordoch, and Shimon Schuldiner*

Department of Biological Chemistry, Alexander Silberman Institute of Life Sciences, Hebrew University of Jerusalem, Jerusalem, Israel

Received 25 May 2005/Accepted 17 August 2005

Multidrug transporters are ubiquitous proteins, and, based on amino acid sequence similarities, they have been classified into several families. Here we characterize a cluster of archaeal and bacterial proteins from the major facilitator superfamily (MFS). One member of this family, the vesicular monoamine transporter (VMAT) was previously shown to remove both neurotransmitters and toxic compounds from the cytoplasm, thereby conferring resistance to their effects. A BLAST search of the available microbial genomes against the VMAT sequence yielded sequences of novel putative multidrug transporters. The new sequences along with VMAT form a distinct cluster within the dendrogram of the MFS, drug-proton antiporters. A comparison with other proteins in the family suggests the existence of a potential ion pair in the membrane domain. Three of these genes, from *Mycobacterium smegmatis*, *Corynebacterium glutamicum*, and *Halobacterium salinarum*, were cloned and functionally expressed in *Escherichia coli*. The proteins conferred resistance to fluoroquinolones and chloramphenicol (at concentrations two to four times greater than that of the control). Measurement of antibiotic accumulation in cells revealed proton motive force-dependent transport of those compounds.

Multidrug resistance is an increasing problem in antimicrobial therapy as well as in treatment of tumors. One of the most common mechanisms of resistance is removal of toxic compounds from the cell, by drug and multidrug transporters (8, 26). Multidrug transporters are ubiquitous proteins, and, based on amino acid sequence similarities, they have been classified into several families. Some of these proteins utilize primary energy source and their activity depends on ATP (ABC transporters) while others utilize secondary energy sources by coupling their activity to the movement of protons down a concentration gradient (19, 27).

The vesicular monoamine transporter (VMAT) catalyzes the accumulation of neurotransmitters in organelles in exchange for two protons (34). Besides its known function, VMAT was shown to protect the cell from the deleterious effect of toxic compounds by lowering their concentrations in the cytoplasm (18). In addition, the range of substrates recognized by VMAT is very wide and led to the suggestion that it behaves as a multidrug transporter (41). Phylogenetic analysis showed that VMAT proteins are evolutionary related to drug transporters and multidrug transporters of the Major facilitator superfamily (MFS) (32, 34). Like most MFS transporters, VMAT consists of 12 putative transmembrane segments ordered in two lobes of six-helix bundles. A feature that distinguishes VMAT proteins from other drug transporters and multidrug transporters of the MFS is a long loop between transmembrane segments TM1 and TM2 that contains glycosylation sites (34).

Mechanistic understanding of membrane proteins is limited by the difficulties in obtaining structural data. These problems stem mainly from difficulties in expressing, purifying, and crystallizing membrane proteins. One of the approaches suggested for structural studies of low-expression mammalian membrane proteins is to study their bacterial and archaeal homologues. Successful examples of this approach can be found in studies of potassium and chloride channels from different sources (4, 5, 13, 14). The high-resolution structures of the bacterial homologues provided an invaluable insight on many aspects of substrate recognition and transport through biological channels. The high-resolution structures of two bacterial MFS proteins were solved: LacY, the lactose permease (1), and GlpT, the phosphate, glycerol 3-phosphate antiporter (10). Although the sequence similarity of these proteins is low (~20% identity), their folds are highly similar. Based on those structures, a model for VMAT was constructed that is in agreement with experimental data (37).

The fold conservation in the MFS proteins and the intriguing connection between multidrug transporters of the MFS and the vesicular neurotransmitter transporters led us to identify and characterize multidrug transporters that are related to VMAT. A BLAST search of the available microbial genomes against the VMAT sequence identified several putative proteins related to VMAT with low but significant similarity (<25% identity). We cloned three of the closest homologues and expressed them in *Escherichia coli* cells. We report here the functional expression and characterization of three new multidrug transporters from three microorganisms: *Mycobacterium smegmatis*, *Corynebacterium glutamicum*, and *Halobacterium salinarum*.

MATERIALS AND METHODS

Sequence analysis. BLAST search using the rVMAT2 sequence as query against the database of the available microbial genomes was done using the NCBI server (http://www.ncbi.nlm.nih.gov/). In order to find more family members the closest sequences derived from the initial BLAST were used for an additional BLAST search in the available databases (2). The derived sequences

* Corresponding author. Mailing address: Department of Biological Chemistry, Alexander Silberman Institute of Life Sciences, Hebrew University of Jerusalem, Jerusalem, Israel. Phone: 972-2-6585992. Fax: 972-2-5634625. E-mail: Shimon.Schuldiner@huji.ac.il.

TABLE 1. Primers used for cloning the homologues

Homologue	Primer	Sequence	Enzyme
CGmdr	Forward	GGTACCCGGGCATATGTTAACTCAAAAAATAGAATTAGAG	NdeI
CGmdr	Reverse	CCGCTCGAGAAGCTTCAGAATTCTACCTGCTCGACTTTCG	EcoRI
HSmdr	Forward	GGTACCCGGGCATATGGGATTGTTGGATACGGATCG	NdeI
HSmdr	Reverse	CCGCTCGAGAAGCTTCAGAATTCGTCACCCGTCGACG	EcoRI
MSmdr	Forward	CGCGGTACCCGGGCATATGGTTCGCCGCGCGGCCGTC	NdeI
MSmdr	Reverse	GCCGCTCGAGAAGCTTCAGAATTCGGGCACCTCGCCGCC	EcoRI

were compared using ClustalW (36) and a representative dendrogram was drawn using the Njplot software (29). Consensus sequences were detected and presented using the GeneDoc software (25) Hydropathic analysis of the sequences was done with TMHMM program (38).

Bacterial strains and plasmids. *E. coli* TA15 (7), JM109 (40), C41 (21), and BL21 and HMS174 (Stratagene, La Jolla, Calif.) were used throughout this work. The pT7-7-Myc-His vector was obtained by removing the *emrE* gene from vector pT7-7-EmrE-Myc-His (23) with restriction enzymes NdeI and EcoRI (New England Biolabs, Beverly, MA). Homologues of interest were cloned by PCR using genomic DNA from *H. salinarum*, *M. smegmatis*, and *C. glutamicum* as templates (provided by M. Mevarech, Department of Microbiology, Tel Aviv University, H. Bercovier, Hadasah Medical School, Hebrew University of Jerusalem, and R. Kraemer, Institute of Biochemistry, University of Cologne, Cologne, Germany, respectively).

Primers (Table 1) were designed to overlap the ends of the genes and included sites for restriction enzymes NdeI and EcoRI. The genomes *of H. salinarum* and *C. glutamicum* are of high GC content and a successful PCR could only be achieved using a GC-rich PCR kit (Roche Diagnostics, GmbH, Mannheim, Germany) with an annealing temperature of 58°C. Each homologue was cloned into the pT7-7-Myc-His vector. The plasmids obtained were named pT7-7 HSmdr for the *H. salinarum* homologue, pT7-7 MSmdr for the *M. smegmatis* homologue, pT7-7 CGmdr for the *C. glutamicum* homologue.

Resistance to toxic compounds. Preliminary screens for resistance were done by disk diffusion susceptibility test on inoculated soft agar plates. A 100-μl sample of late-stationary-phase cultures *of E. coli* JM109 transformed with pT7-7(−), pT7-7 HSmdr, pT7-7 MSmdr, and pT7-7 CGmdr were used to inoculate 10 ml of warm soft LB-agar (0.7% Agar) (33) that was then poured into plates. Antibiotic disks (Mast Diagnostics GmbH. Reinfeld, Germany) were placed on the soft agar layer. After 18 h, growth inhibition zones, created by the different antibiotics, were compared between the control [pT7-7(−)] and the cells expressing the homologues. The following antibiotics were examined: amikacin, ceftazidime, gentamicin, imipenem, meropenem, ofloxacin, tazocin, timentin, ampicillin, cephalothin, colistin sulfate, streptomycin, sulfatriad, tetracycline, cotrimoxazole, amoxicillin-clavulanic acid, oxacillin, erythromycin, vancomycin, fusidic acid, cefuroxime, nitrofurantoin, ciprofloxacin, and amoxicillin.

Resistance to chloramphenicol and ofloxacin was studied in more detail in liquid medium: *E. coli* JM109 expressing the homologues was grown at 37°C in LB containing ampicillin (100 μg/ml) to mid-logarithmic phase to an approximate optical density at 600 nm (OD_{600}) of 0.8. The logarithmic cultures were diluted to give OD_{600} of 0.05 and grown in the presence of chloramphenicol or ofloxacin at different concentrations. Growth was assessed by OD_{600} measurements after 8 h. Chloramphenicol was dissolved in 100% ethanol to 25 mg/ml. Ofloxacin (LKT Laboratories, St. Paul, MN) was dissolved in sodium acetate buffer (20 mM, pH 4) at a concentration of 4 mg/ml. Both antibiotics were diluted in growth medium before adding to the bacterial culture.

Transport of chloramphenicol and ofloxacin. Transport of antibiotics in whole cells was assessed by measuring their accumulation, essentially as described before (6). Late-stationary-phase cultures were used to inoculate ampicillin-supplemented LB to an OD_{600} of 0.02. Bacteria were grown to logarithmic phase, harvested, and washed once with 50 mM potassium phosphate buffer at pH 7.1. The pellet was resuspended with the same buffer to an OD_{420} of 20 and kept on ice until assayed: The assay started with 5 min incubation of the cells with 10 mM glucose at 30°C followed by addition of the antibiotics and incubation for 30 seconds to 10 min. The reaction was stopped by addition of 2 ml of ice-cold buffer (50 mM potassium phosphate buffer) and rapid filtration through GF/C glass microfiber filters (Whatman, Maidstone, England), and after filtration the filters were washed with ice cold buffer.

To obtain the equilibration value for all strains, accumulation of ofloxacin and chloramphenicol was also measured in the presence of 0.5 mM of the proton uncoupler carbonyl cyanide *m*-chlorophenylhydrazone (CCCP) for 10 min. The ratio between accumulation with and without CCCP was calculated. A decrease in that ratio in bacteria expressing the putative multidrug resistance (MDR) proteins suggests the activity of a proton motive force-dependent efflux system.

The ofloxacin accumulation test was carried with 200 μl of the resuspended culture and was done essentially as described (22) with modifications. After rapid filtration the filters were incubated for 18 h in 1 ml glycine-HCl buffer (100 mM, pH 3), and ofloxacin levels in the buffer were assessed by fluorescence measurement using a PerkinElmer fluorimeter (Luminescence Spectrometer LS-50) with exciting light at 295 nm and emission at 495 nm. The maximum fluorescence signal after addition of CCCP was ~110 and it was fitted to accumulation of 36 ng ofloxacin. The chloramphenicol accumulation test was carried with 50 μl of the resuspended culture and was done by measuring the accumulated [^{3}H]chloramphenicol (American Radiolabeled Chemicals, St. Louis, MO) at a final concentration of 0.5 μM chloramphenicol and specific activity of 0.5 Ci/mmol (200,000 dpm total in the reaction). The maximum signal obtained after addition of CCCP was 35,000 dpm.

In both cases, the level of free antibiotics bound to the filter was measured and subtracted from the antibiotics accumulated in the bacteria. The experiments were carried out in duplicates and repeated at least twice.

Protein expression. The expression of the three cloned homologues was examined in a strain designed for protein expression: *E. coli* HMS174 cells were transformed with the three plasmids and expression of the proteins was examined. A late-stationar-phase culture was used to inoculate 2XYT medium (33) supplemented with 100 μg/ml ampicillin to yield an OD_{600} of 0.1. The culture was incubated at 37°C under aerobic conditions until an OD_{600} of 0.9, at which time isopropyl-β-D-thiogalactopyranoside (IPTG) was added to a final concentration of 1 mM. Two hours later, the cells were harvested by centrifugation and washed once with lysis buffer (150 mM NaCl, 15 mM Tris, pH 7.5, 250 mM sucrose) before further handling or storage at −70°C.

Membranes were prepared using lysozyme and hypo-osmolarity for disruption of the cells as described (15) except that the volumes used were modified.

Detection of the protein in the crude membranes was done by Western blotting with mouse anti-Myc as a primary antibody and mouse anti-rabbit immunoglobulin-horseradish peroxidase as a secondary antibody (Invitrogen Carlsbad, Calif.). Detection of the secondary antibody was done with chemiluminescence Super-signal kit (Pierce, Rockford, IL).

Protein purification for SDS-PAGE. Membranes were thawed and solubilized in a denaturing buffer (15 mM Tris-Cl pH 7.5, 150 mM NaCl, 2% sodium dodecyl sulfate [SDS], and 6 M urea) at room temperature for 30 min. The solubilized membranes were then centrifuged (244,000 × g, 20 min) to remove the nonsoluble fraction. The supernatant was incubated with Ni^{2+}-nitrilotriacetic acid-agarose beads (QIAGEN, GmbH, Hilden, Germany) for 1 h, with 10 mM imidazole. The beads were then washed with denaturing buffer containing imidazole (30 mM). Elution of the protein from the beads was done with sample buffer containing 300 mM imidazole.

RESULTS

Sequence homology and analysis. The vesicular monoamine transporter facilitates the accumulation of different compounds into vesicles using proton motive force. This protein was shown to belong to the drug/H^+ antiporters (DHA12) of the major facilitator superfamily. This family is divided into five clusters and VMAT is part of a separate branch in one of them (27). A BLAST search of rVMAT2 against the available bacterial genomes (May 2005) revealed relatives with low but significant identity to VMAT; the closest of them had up to 24% identity and *e* values up to $\sim 10^{-12}$. In this BLAST search more than 15 uncharacter-

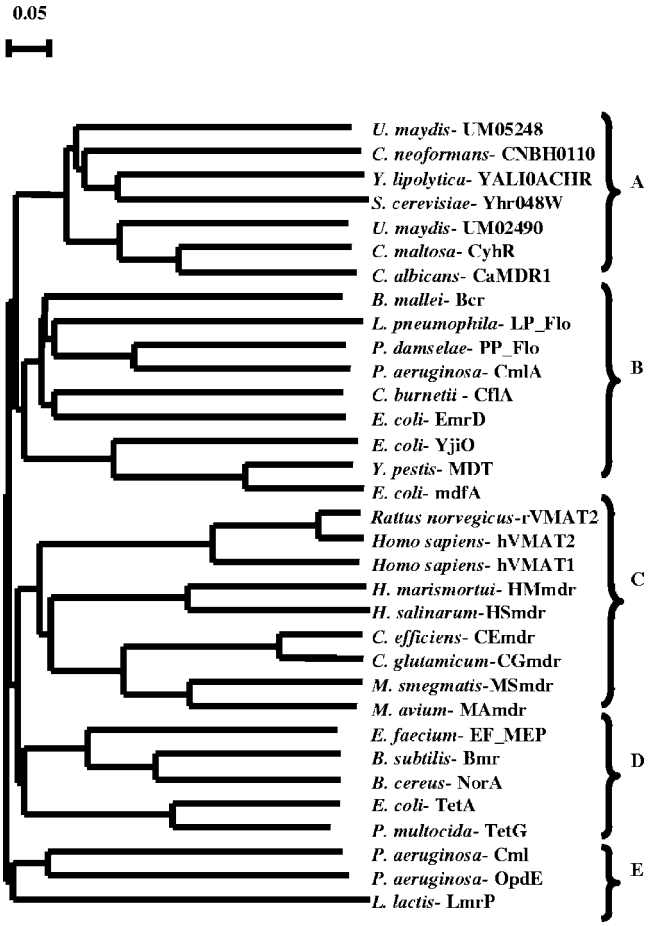

FIG. 1. Dendrogram of the main clusters of the DHA12 family. The tree consists of representatives from each cluster in the DAH12 family. Cluster A consists of drug and multidrug transporters from yeast and fungi. The rest of the clusters consist of sequences from different bacteria and archaea. The novel multidrug transporters (CGmdr, MSmdr, and HSmdr) form differentiated branches in the same cluster with VMAT (cluster C). The sources of the sequences in the dendrogram are as follows. Cluster A: UM05248—*Ustilago maydis*, CNBH0110—*Cryptococcus neoformans*, YALI0ACHR—*Yarrowia lipolytica*, Yhr048W—*Saccharomyces cerevisiae*, UM02490—*Ustilago maydis*, CyhR—*Candida maltosa*, and CaMDR1—*Candida albicans*. Cluster B: Bcr—*Burkholderia mallei*, LP_Flo—*Legionella pneumophila*, PP_Flo—*Photobacterium damselae*, CmlA—*Pseudomonas aeruginosa*, CflA—*Coxiella burnetii*, EmrD—*Escherichia coli*, MdfA—*Escherichia coli*, MDT—*Yersinia pestis* biovar Medievalis, and YjiO—*Escherichia coli*. Cluster C: rVMAT2—*Rattus norvegicus*, hVMAT2—*Homo sapiens*, hVMAT1—*Homo sapiens*, HMmdr—*Haloarcula marismortui*, HSmdr (YfmO2)—*Halobacterium* sp. NRC-1, CEmdr—*Corynebacterium efficiens*, CGmdr—*Corynebacterium glutamicum*, MSmdr—*Mycobacterium smegmatis*, and MAmdr—*Mycobacterium avium*. Cluster D: EF_MEP—*Enterococcus faecium*, Bmr—*Bacillus subtilis*, NorA—*Bacillus cereus*, TetA—*Escherichia coli*, TetG—*Pasteurella multocida*. Cluster E: CmlA—*Pseudomonas aeruginosa*, OpdE—*Pseudomonas aeruginosa*, LmrP—*Lactococcus lactis*.

ized, putative proteins with an *e* value better than 5×10^{-8} were detected.

Phylogenetic analysis of the putative transporters revealed that they are clustered together with VMAT proteins within the DHA12 family (Fig. 1, cluster C). In the figure only some of the homologues are shown for the sake of clarity but three branches are clearly observed: VMATs, archaeal proteins and proteins from *Corynbacterineae*. The *Corynbacterineae* branch is divided into two distinct subgroups one from *Corynebacterium* and one from *Mycobacterium*.

Hydropathic analysis of the new sequences revealed, as usual for MFS proteins, 12 putative transmembrane domains divided into two halves by a long cytoplasmic loop between TM6 and TM7. In Fig. 2A, a predicted two-dimensional model of MSmdr is shown.

The multiple sequence alignment of cluster C revealed several conserved regions (Fig. 2B) mainly in the N-terminal lobe (TM1, TM2, L2–3, L3–4, TM4, L4–5, and TM5) and to a lesser extent in the C-terminal lobe (L8–9 and TM11). Motifs defined by Paulsen et al. (27) for the entire DHA12 family were compared with motifs detected in this cluster. As expected, the motifs are similar between the DHA12 and members of its subfamily in cluster C but there are some characteristics that are specific for cluster C: motif D2 is located in TM1 (Fig. 2B). The most distinct feature of this motif is the two adjacent prolines separated by two residues. In the models created for two transporters of this family (37) the conserved prolines are located close to the distortion of TM1 suggesting a structural role for this motif. Generally, motif D2 is conserved in cluster C as it is in the entire family but the archaeal branch misses the first P of the motif (Fig. 2).

Motif A is located in a conserved loop between TM2 and 3 (Fig. 2B) and has been attributed a structural role (reviewed in (27) and (30). In cluster C the motif is hardly changed and it begins with a highly conserved proline three residues prior to the conserved glycine. The conserved aspartate downstream from the glycine may be changed in cluster C to glutamate or polar residues (glutamine and asparagine) (Fig. 2).

Motif B is located in TM4 (Fig. 2) and was suggested to be involved in proton transfer or recognition (28). This RXXXG motif is conserved in the whole family and it was shown that a mutation in the arginine of this motif resulted in an inactive form of the tetracycline transporter, TetAB (11). In cluster C, this motif is conserved and expanded at the N terminus with a conserved region that is unique to this cluster (Fig. 2).

Motif C is located in TM5 (Fig. 2) and its main feature is a sequence of three glycines separated from each other by three residues (GxxxGxxxG). The spacing between the glycines may reflect one helix turn and that may point towards a structural role. This motif is conserved in cluster C, and in addition, 15 residues upstream from it, there is an additional motif (C-15) completely conserved in this cluster and absent from other clusters (RgrXXgX) (Fig. 2).

Motif G is located in TM11 (Fig. 2B) and it is a variation of motif C in TM5, its symmetric counterpart in the N-terminal lobe. In cluster C some additional conserved residues are located downstream from this motif.

In the earlier analyses no other variations of motifs were found in corresponding regions of the DHA12 family (27), but when examining the existence of such variants in other TMs in cluster C, a variation of motif A (TM2) is found in TM8 (Fig. 2), and is referred to as motif A2 (Fig. 2B).

Other structural information can be hinted from the suggestion of a conserved fold in the MFS proteins. The structural model of VMAT described an ion pair between the conserved aspartate in TM11 and the conserved lysine in TM2 (37). This

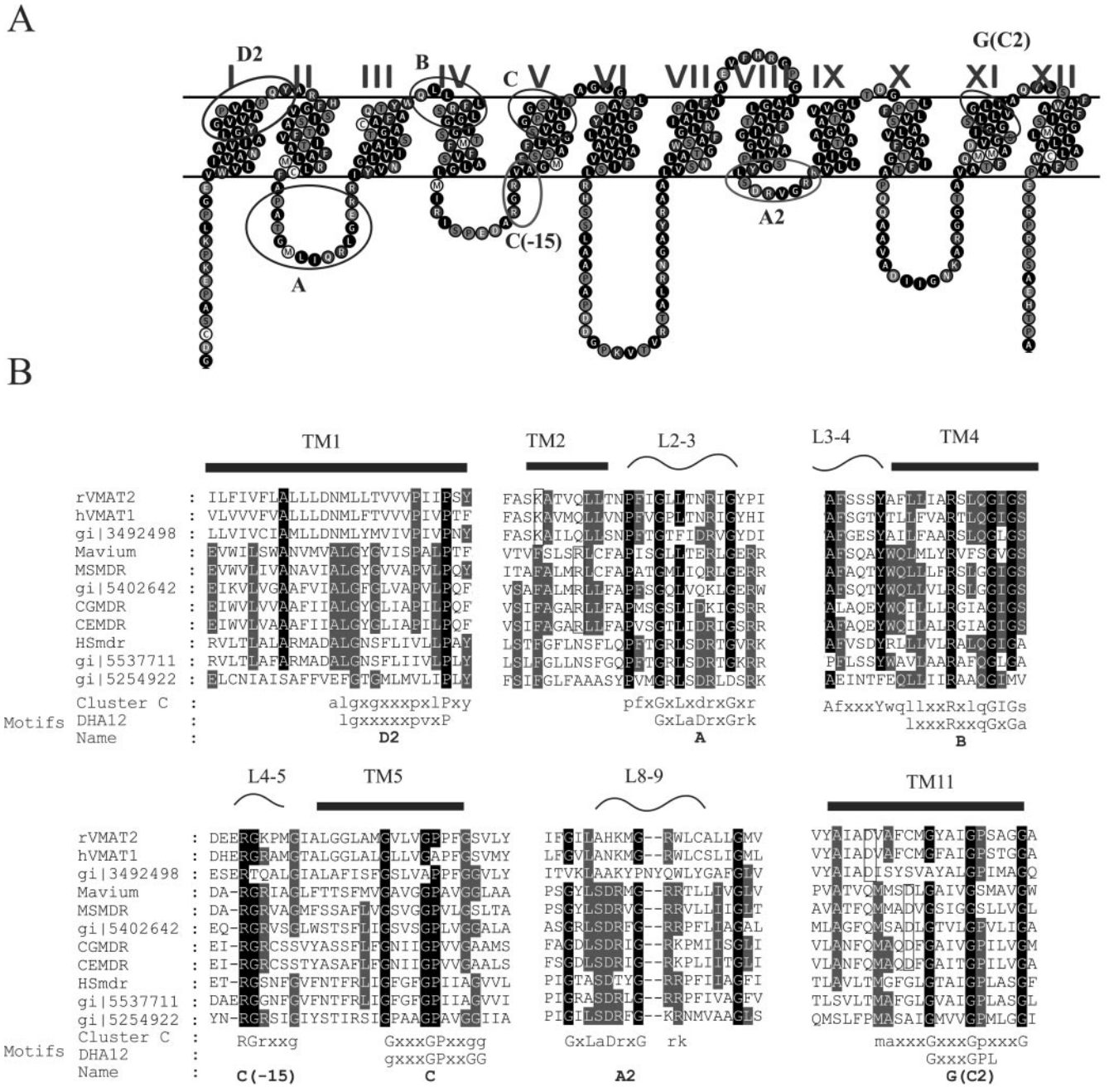

FIG. 2. Sequence analysis of cluster C. A. A representative topology suggested for DHA12 proteins contains 12 transmembrane domains divided into two halves by a long cytoplasmic loop between TM6 and TM7. The topology shown is that of MSmdr. Motifs from the DHA12 family are marked with black circles and motifs specific for cluster C are marked with gray circles. B. Conserved regions in the sequence alignment of cluster C. At the bottom of the alignment are consensus sequences in which capital letters represent frequency occurrence greater than 90% (dark shading) and small capitals represent frequency occurrence greater than 50% (light gray shading). The consensuses are compared with the DHA12 motifs defined by Paulsen et al. (27). The arrows above the sequences point to residues involved in putative ion pairs (open rectangles).

ion pair is supported by experimental data (20). In the *Corynebacterineae* branch this aspartate is shifted one helix turn further towards the C terminus of the TM than in VMAT (Fig. 2B). Correspondingly, in TM2 an arginine of the *Corynebacterineae* branch is located exactly one helix turn from the conserved lysine (Fig. 2B). This finding strongly supports the above proposal for an interaction between the charged residues in TM2 and TM11. This suggestion implies that the charged residues in TM2 and TM11 cannot be buried in the membrane without their opposite charge, and as a further support for this notion in the archaeal branch, both charged residues are absent (Fig. 2B).

Representatives from each of the three branches of cluster C were cloned and expressed in *E. coli*: from an unfinished fragment of the genome of *Mycobacterium smegmatis*, MSmdr (starting base 2211693); from *Corynebacterium glutamicum*,

CGmdr (accession number NP_600365); and from the archaeon *Halobacterium salinarum*, HSmdr (also called YfmO2, accession number NP_279495).

Phenotype of the novel homologues. The novel DHA12 proteins were tested for drug resistance. The phenotypic characterization of drug resistance in strains expressing the proteins was done using disk diffusion susceptibility tests with 25 drugs as described in Materials and Methods. *E. coli* cells harboring plasmids with the homologues exhibited a limited spectrum of resistance (data not shown). Among the compounds tested, the most distinct resistance was observed for ciprofloxacin and ofloxacin. The two homologues from the *Corynebacterineae* (MSmdr and CGmdr) also conferred resistance to chloramphenicol.

To further characterize the phenotype, growth of *E. coli* JM109 cells carrying plasmids with or without the homologues in LB medium containing ofloxacin or chloramphenicol at different concentration was examined (Fig. 3A and B). CGmdr- and MSmdr-expressing strains were equally resistant to both chloramphenicol and ofloxacin. HSmdr conferred less resistance to chloramphenicol and slightly more resistance to ofloxacin than the other homologues. In this assay, the approximate 50% inhibitory concentration (IC_{50}) values for chloramphenicol are 4 μg/ml for CGmdr and MSmdr, 2 μg/ml for HSmdr, and 1 μg/ml for the control (Fig. 3A). The IC_{50} value for the three homologues is ~200 ng/ml, while for the control strain it is ~50 ng/ml (Fig. 3B).

Transport of chloramphenicol and ofloxacin by the bacterial homologues. Bacteria expressing H^+/drug antiporters are expected to remove the drug in a process dependent on the proton electrochemical gradient. Thus, ofloxacin and chloramphenicol transport into whole cells was examined in the presence or absence of the proton uncoupler CCCP. In the presence of CCCP accumulation levels were very similar in all strains, representing the equilibration value for the two compounds (data not shown). In the absence of CCCP, accumulation levels differed significantly among the different strains. The data in Fig. 4 are presented relative to uptake in the presence of CCCP.

The control strain exhibited the highest uptake for both chloramphenicol and ofloxacin. Cells expressing HSmdr accumulated ofloxacin twofold less than control. In CGmdr- and MSmdr-expressing cells ofloxacin was accumulated to a level of two-thirds of the control. Chloramphenicol accumulation in HSmdr-expressing cells was two-thirds of that observed in the control cells while cells expressing MSmdr and CGmdr accumulated to a level of about one third of the control (Fig. 4B). The uptake profile of the novel multidrug transporters is in good accordance with their resistance profile. The result supports the contention that transport catalyzed by the three proteins is driven by proton electrochemical gradient.

Protein expression. To characterize the system at the protein level the three putative transporters (tagged with Myc-His) (23) were expressed in *E. coli* HMS174. To test expression levels, membranes from known volumes of IPTG-induced cultures were solubilized in denaturing buffer (1% SDS, 6 M urea, 15 mM Tris-Cl, pH 7.2, 150 mM NaCl), purified on Ni^{+2}-nitrilotriacetic acid beads and analyzed by SDS-polyacrylamide gel electrophoresis (PAGE).

As judged by Coomassie stain of the purified protein, the expression level of CGmdr was 20 times higher than that of MSmdr and ~500 times higher than that of HSmdr (Fig. 5A). While hardly detectable by Coomassie staining HSmdr from the crude membrane fraction was detected by Western blotting with an anti-Myc antibody. CGmdr and MSmdr (from 10- and 5-fold less membrane protein than HSmdr, respectively) were also detected by Western blot and displayed similar apparent molecular weights (Fig. 5B). The calculated sizes of the three proteins are 42.3, 47.7, and 42.7 kDa for CGmdr, MSmdr, and HSmdr, respectively. As commonly seen for many membrane proteins, the apparent sizes detected by SDS-PAGE are lower than expected but are consistent with the fact that MSmdr is the largest of the three and the others have very similar molecular masses. For CGmdr, which is expressed to the highest levels, a higher-molecular-weight form that corresponds to a dimer is apparent in both SDS-PAGE and Western blotting.

DISCUSSION

In this study, we describe a basic characterization of three proteins encoded by genes belonging to a cluster of the DHA12 family of MFS transporters. A BLAST search of the available microbial genomes with VMAT as an input yielded several novel, uncharacterized sequences that are closer to VMAT than any other reported proteins from bacteria and archaea. Although the similarity of the new sequences to VMAT is not very high (~20%), there are several conserved motifs that characterize this cluster. In the DHA12 family five major clusters have been previously identified and several of the proteins in the four other clusters have been studied quite intensively (27). However, we are not aware of any study of proteins in the cluster defined by VMAT. In this cluster three differentiated branches with sequence similarities and differences can be distinguished: one of the mammalian proteins, one from a member of the *Corynebacterineae*, and the third from an archaeon. All of the motifs identified by Paulsen et al. (27) are conserved in cluster C and some specific features have been identified here, notably, a putative ion pair in the membrane domain is hinted by comparison with other members of the family.

Two putative protein sequences from the *Corynebacterineae* branch, MSmdr from *Mycobacterium smegmatis* and CGmdr from *Corynebacterium glutamicum*, and one from the archaeal branch, HSmdr from *Halobacterium salinarum*, were cloned and expressed in *E. coli*. The three proteins were expressed and targeted to the membrane and conferred resistance to two quinolones and to chloramphenicol. Although the chloramphenicol resistance conferred by CGmdr and MSmdr is lower than that conferred by other multidrug transporters, the quinolone resistance conferred by the three homologues is in the same range as that conferred by other DHA12 drug transporters. For example, the ciprofloxacin level that may be endured by MdfA-expressing cells is four times higher than that of the control (6). The MIC of ofloxacin for *E. coli* overexpressing NorA is four times higher than for its control (24).

Transport of chloramphenicol and ofloxacin by *E. coli* JM109 expressing the new transporters was measured in the presence and absence of CCCP. The effect of CCCP on transport suggests that, as predicted for an MFS transporter, the process is driven by the proton electrochemical gradient gen-

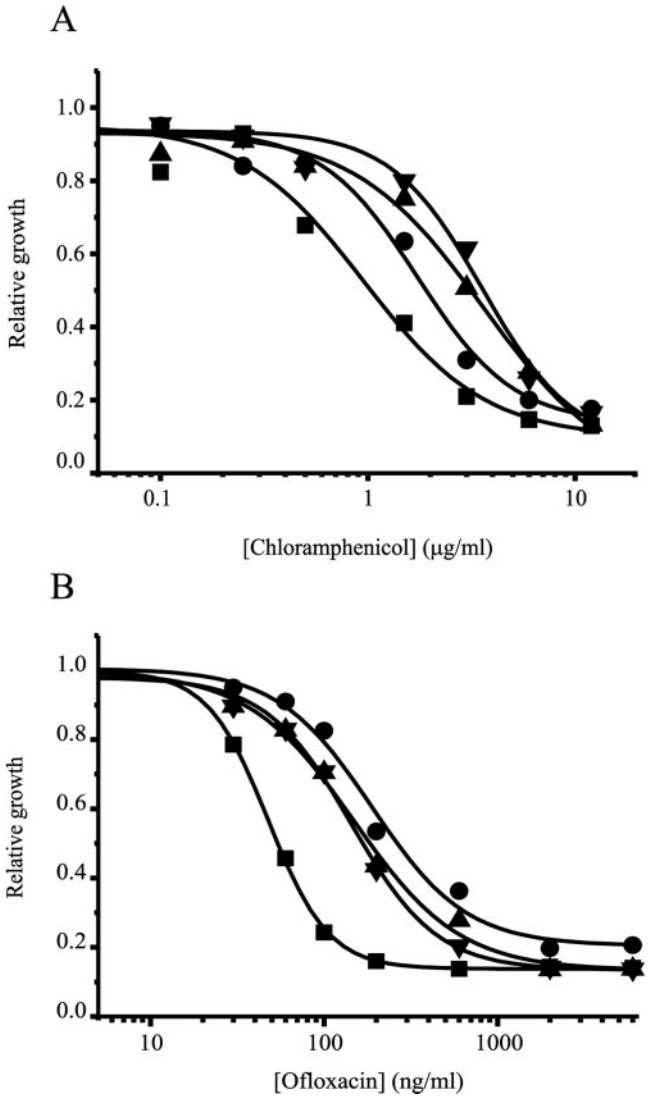

FIG. 3. Resistance to toxic compounds. The growth of *E. coli* JM109 expressing CGmdr (▼), MSmdr (▲), HSmdr (●), and the control (■) in the presence of the indicated concentrations of chloramphenicol (A) or ofloxacin (B). Bacterial growth after 8 h is shown relative to growth without antibiotics. The experiment was repeated three times. One representative experiment is shown.

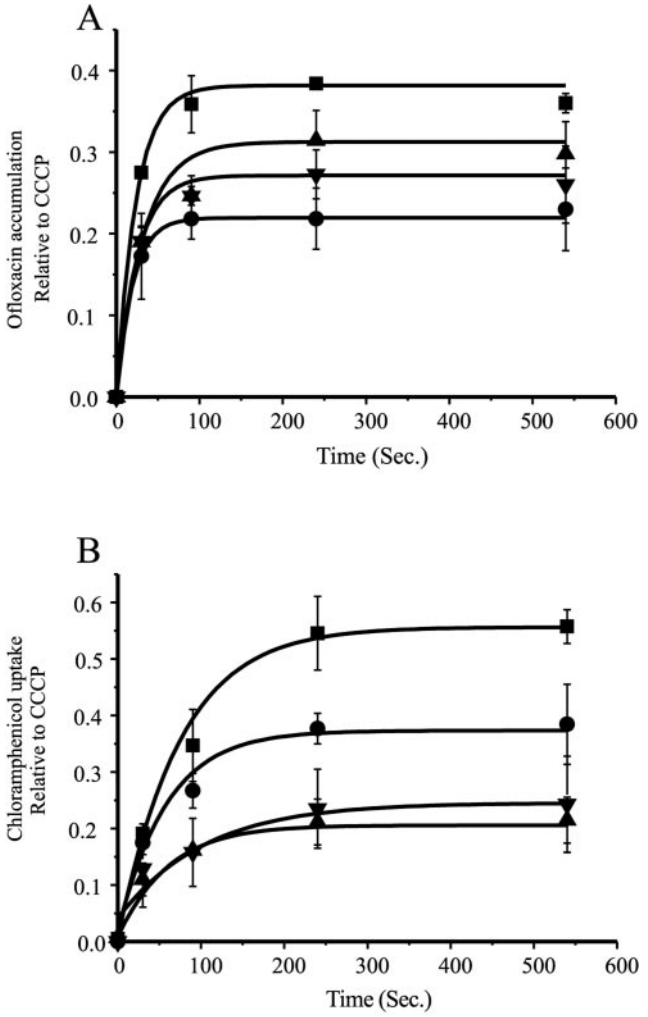

FIG. 4. Antibiotic accumulation in *E. coli.* A—Ofloxacin uptake in JM109 bearing pT7-7 CGmdr (▼), pT7-7 MSmdr (▲), pT7-7 HSmdr (●), and the control (■). Data represent relative uptake (uptake divided by the maximum uptake in the presence of CCCP). Ofloxacin was added to 200 μl of bacterial culture (OD_{420} = 20) to reach the final concentration of 30 μM. At the indicated times bacteria were separated from the medium by rapid filtration and ofloxacin was measured by fluorescence. CCCP was added to parallel tubes to a final concentration of 0.5 mM. B— Chloramphenicol uptake in the same strains of JM109 relative to uptake after addition of CCCP. Chloramphenicol uptake was measured as described above for ofloxacin except that the latter was replaced with [^{3}H]chloramphenicol at a final concentration of 0.5 μM. The experiment was repeated three times. One representative experiment is shown.

erated across the cytoplasmic membrane by primary pumps. Since resistance is also observed at alkaline pH values (data not shown) where the only driving force is the membrane potential, the results might suggest that the efflux is an electrogenic process involving the exchange of more than one proton with a substrate molecule (for detailed discussion see references 16 and 31).). There is a good agreement between drug resistance and the efflux activity measured here. CGmdr and MSmdr conferred resistance to both chloramphenicol and ofloxacin, and both transporters removed these compounds to similar levels. A relatively weak resistance to chloramphenicol was detected in cells expressing HSmdr and the ability of these cells to remove chloramphenicol was significantly lower than that of cells expressing the other transporters. On the other hand the quinolone resistance conferred by HSmdr, similar to that conferred by the other two homologues, was accompanied by efficient ofloxacin removal.

Our knowledge of the function of drug transporters in archaea and in *C. glutamicum* and related organisms is very limited. The studies presented here provide the first report of an MFS drug transporter for *Halobacterium* sp. strain NRC1. In the case of *C. glutamicum* there is, as far as we know, only one report of an MFS drug transporter (12). CGmdr is highly similar to two uncharacterized open reading frames in two other actinobacteria, *Corynebacterium efficiens* (70% identity, starting at base 1262385) and *Nocardia farcinica* (40% identity,

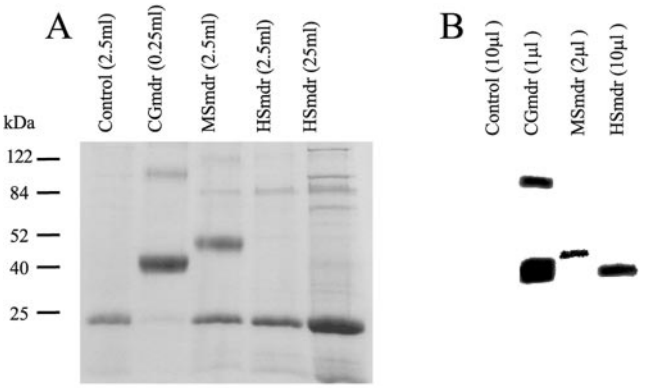

FIG. 5. Expression of the transporters in HMS174 strain. *E. coli* HMS174 cells carrying a pT7-7 plasmid with the gene coding for each of the homologues were used for expression. After harvesting, membranes were prepared as described in Materials and Methods and solubilized in 2% SDS–6 M urea. A. Different culture volumes were used for protein purification of SDS-Urea solubilized membranes with Ni-nitrilotriacetic acid beads as described in Materials and Methods. CGmdr was purified from 250 μl culture, MSmdr, HSmdr, and the control from 2.5 ml, and an additional HSmdr preparation from 25 ml culture. B. Total membranes were solubilized in denaturing buffer, separated by SDS-PAGE, and underwent Western blot analysis with rabbit anti-Myc as the primary antibody. The samples shown are from 1 μl CGmdr, 2 μl MSmdr, and 10 μl HSmdr membranes (25 mg protein/ml).

starting at base 4621748). Expression in the natural hosts was not studied here, but the existence of close homologues in other bacteria hints of a natural role which may involve multidrug transporter activity.

Drug resistance in mycobacteria has been studied quite extensively because of the fact that even now in the 21st century, *Mycobacterium tuberculosis* is still the deadliest single killer according to a World Health Organization report (39). Mycobacteria are gram-positive bacteria intrinsically resistant to a variety of antibacterials. Several mycobacterial MFS multidrug transporters have been reported in *M. tuberculosis* and *M. smegmatis* (17). Inactivation of chromosomal genes in *M. smegmatis* points to several transporters that may mediate the intrinsic drug resistance (17). The *M. smegmatis* transporter characterized here is a homologue (50% identity) of an open reading frame in *M. avium* (unfinished genome, starting at base 5080617).

ACKNOWLEDGMENTS

This work was supported by grant 2003-309 from the United States-Israel Binational Science Foundation, Jerusalem, Israel, and from the Center for Innovation in Membrane Protein Production (P50 GM73210). Shimon Schuldiner is Mathilda Marks-Kennedy Professor of Biochemistry at the Hebrew University of Jerusalem.

REFERENCES

1. **Abramson, J., I. Smirnova, V. Kasho, G. Verner, H. R. Kaback, and S. Iwata.** 2003. Structure and mechanism of the lactose permease of *Escherichia coli*. Science **301:**610–615.
2. **Altschul, S. F., T. L. Madden, A. A. Schaffer, J. Zhang, Z. Zhang, W. Miller, and D. J. Lipman.** 1997. Gapped BLAST and PSI-BLAST: a new generation of protein database search programs. Nucleic Acids Res. **25:**3389–3402.
3. **Bradford, M. M.** 1976. A rapid and sensitive method for the quantitation of microgram quantities of protein utilizing the principle of protein-dye binding. Anal. Biochem. **72:**248–254.
4. **Doyle, D. A., J. Morais Cabral, R. A. Pfuetzner, A. Kuo, J. M. Gulbis, S. L. Cohen, B. T. Chait, and R. MacKinnon.** 1998. The structure of the potassium channel: molecular basis of K+ conduction and selectivity. Science **280:**69–77.
5. **Dutzler, R., E. B. Campbell, M. Cadene, B. T. Chait, and R. MacKinnon.** 2002. X-ray structure of a ClC chloride channel at 3.0 A reveals the molecular basis of anion selectivity. Nature **415:**287–294.
6. **Edgar, R., and E. Bibi.** 1997. MdfA, an *Escherichia coli* multidrug resistance protein with an extraordinarily broad spectrum of drug recognition. J. Bacteriol. **179:**2274–2280.
7. **Goldberg, E. B., T. Arbel, J. Chen, R. Karpel, G. A. Mackie, S. Schuldiner, and E. Padan.** 1987. Characterization of a Na+/H+ antiporter gene of *Escherichia coli*. Proc. Natl. Acad. Sci. USA **84:**2615–2619.
8. **Gottesman, M. M., I. Pastan, and S. V. Ambudkar.** 1996. P-glycoprotein and multidrug resistance. Curr. Opin. Genet. Dev. **6:**610–617.
9. **Gutman, N., S. Steiner-Mordoch, and S. Schuldiner.** 2003. An amino acid cluster around the essential Glu-14 is part of the substrate-and proton-binding domain of EmrE, a multidrug transporter from *Escherichia coli*. J. Biol. Chem. **278:**16082–16087.
10. **Huang, Y., M. J. Lemieux, J. Song, M. Auer, and D. N. Wang.** 2003. Structure and mechanism of the glycerol-3-phosphate transporter from *Escherichia coli*. Science **301:**616–620.
11. **Iwaki, S., N. Tamura, T. Kimura-Someya, S. Nada, and A. Yamaguchi.** 2000. Cysteine-scanning mutagenesis of transmembrane segments 4 and 5 of the Tn10-encoded metal-tetracycline/H+ antiporter reveals a permeability barrier in the middle of a transmembrane water-filled channel. J. Biol. Chem. **275:**22704–22712.
12. **Jager, W., J. Kalinowski, and A. Puhler.** 1997. A *Corynebacterium glutamicum* gene conferring multidrug resistance in the heterologous host Escherichia coli. J. Bacteriol. **179:**2449–2451.
13. **Jiang, Y., A. Lee, J. Chen, M. Cadene, B. T. Chait, and R. MacKinnon.** 2002. Crystal structure and mechanism of a calcium-gated potassium channel. Nature **417:**515–522.
14. **Jiang, Y., A. Lee, J. Chen, V. Ruta, M. Cadene, B. T. Chait, and R. MacKinnon.** 2003. X-ray structure of a voltage-dependent K^+ channel. Nature **423:**33–41.
15. **Kaback, H. R.** 1971. Bacterial membranes. Methods Enzymol. **22:**99–120.
16. **Lewinson, O., J. Adler, G. J. Poelarends, P. Mazurkiewicz, A. J. Driessen, and E. Bibi.** 2003. The *Escherichia coli* multidrug transporter MdfA catalyzes both electrogenic and electroneutral transport reactions. Proc. Natl. Acad. Sci. USA **100:**1667–1672.
17. **Li, X. Z., L. Zhang, and H. Nikaido.** 2004. Efflux pump-mediated intrinsic drug resistance in *Mycobacterium smegmatis*. Antimicrob. Agents Chemother. **48:**2415–2423.
18. **Liu, Y., D. Peter, A. Roghani, S. Schuldiner, G. G. Prive, D. Eisenberg, N. Brecha, and R. H. Edwards.** 1992. A cDNA that suppresses MPP+ toxicity encodes a vesicular amine transporter. Cell **70:**539–551.
19. **Marger, M. D., and M. H. Saier, Jr.** 1993. A major superfamily of transmembrane facilitators that catalyse uniport, symport and antiport. Trends Biochem. Sci. **18:**13–20.
20. **Merickel, A., H. R. Kaback, and R. H. Edwards.** 1997. Charged residues in transmembrane domains II and XI of a vesicular monoamine transporter form a charge pair that promotes high affinity substrate recognition. J. Biol. Chem. **272:**5403–5408.
21. **Miroux, B., and J. E. Walker.** 1996. Overproduction of proteins in *Escherichia coli*: mutant hosts that allow synthesis of some membrane proteins and globular proteins at high levels. J. Mol. Biol. **260:**289–298.
22. **Mortimer, P. G., and L. J. Piddock.** 1991. A comparison of methods used for measuring the accumulation of quinolones by Enterobacteriaceae, Pseudomonas aeruginosa and *Staphylococcus aureus*. J. Antimicrob. Chemother. **28:**639–653.
23. **Muth, T. R., and S. Schuldiner.** 2000. A membrane-embedded glutamate is required for ligand binding to the multidrug transporter EmrE. EMBO J. **19:**234–240.
24. **Ng, E. Y., M. Trucksis, and D. C. Hooper.** 1994. Quinolone resistance mediated by norA: physiologic characterization and relationship to flqB, a quinolone resistance locus on the *Staphylococcus aureus* chromosome. Antimicrob. Agents Chemother. **38:**1345–1355.
25. **Nicholas, K. B., H. B. Nicholas, Jr, and D. W. Deerfield.** 1997. GeneDoc: analysis and visualization of genetic variation. EMBnet News Online 4. http://acer.gen.tcd.ie/embnet.news/vol4_2.
26. **Nikaido, H.** 1994. Prevention of drug access to bacterial targets: permeability barriers and active efflux. Science **264:**382–388.
27. **Paulsen, I. T., M. H. Brown, and R. A. Skurray.** 1996. Proton-dependent multidrug efflux systems. Microbiol. Rev. **60:**575–608.
28. **Paulsen, I. T., and R. A. Skurray.** 1993. Topology, structure and evolution of two families of proteins involved in antibiotic and antiseptic resistance in eukaryotes and prokaryotes–an analysis. Gene **124:**1–11.
29. **Perriere, G., and M. Gouy.** 1996. WWW-query: an on-line retrieval system for biological sequence banks. Biochimie **78:**364–369.
30. **Putman, M., H. W. van Veen, and W. N. Konings.** 2000. Molecular properties of bacterial multidrug transporters. Microbiol. Mol. Biol. Rev. **64:**672–693.
31. **Rotem, D., and S. Schuldiner.** 2004. EmrE, a multidrug transporter from

Escherichia coli, transports monovalent and divalent substrates with the same stoichiometry. J. Biol. Chem. **279:**48787–48793.
32. **Saier, M. H., Jr., and I. T. Paulsen.** 2001. Phylogeny of multidrug transporters. Semin. Cell Dev. Biol. **12:**205–213.
33. **Sambrook, J., R. D.** 2001. Molecular cloning: a laboratory manual, 3rd ed., vol. 1–3. Cold Spring Harbor Laboratory Press, Cold Spring Harbor,. NY.
34. **Schuldiner, S., A. Shirvan, and M. Linial.** 1995. Vesicular neurotransmitter transporters: from bacteria to humans. Physiol. Rev. **75:**369–392.
35. **Tabor, S., and C. C. Richardson.** 1985. A bacteriophage T7 RNA polymerase/promoter system for controlled exclusive expression of specific genes. Proc. Natl. Acad. Sci. USA **82:**1074–1078.
36. **Thompson, J. D., D. G. Higgins, and T. J. Gibson.** 1994. CLUSTAL W: improving the sensitivity of progressive multiple sequence alignment through sequence weighting, position-specific gap penalties and weight matrix choice. Nucleic Acids Res. **22:**4673–4680.
37. **Vardy, E., I. T. Arkin, K. E. Gottschalk, H. R. Kaback, and S. Schuldiner.** 2004. Structural conservation in the major facilitator superfamily as revealed by comparative modeling. Protein Sci. **13:**1832–1840.
38. **Viklund, H., and A. Elofsson.** 2004. Best alpha-helical transmembrane protein topology predictions are achieved using hidden Markov models and evolutionary information. Protein Sci. **13:**1908–1917.
39. **World Health Organization.** 2005. Global tuberculosis control—surveillance, planning, financing (W.H.O./HTM/TB/2005.349). World Health Organization, Geneva, Switzerland.
40. **Yanisch-Perron, C., J. Viera, and J. Messing.** 1985. Improved M13 phage cloning vectors and host strains: nucleotide sequences of the M13mp18 and pUC19 vectors. Gene **33:**103–119.
41. **Yelin, R., and S. Schuldiner.** 1995. The pharmacological profile of the vesicular monoamine transporter resembles that of multidrug transporters. FEBS Lett. **377:**201–207.